


Spatial-temporal structure functions in Burgers turbulence driven by an Ornstein-Uhlenbeck process

Jin-Han Xie ^{*}

Department of Mechanics and Engineering Science at College of Engineering and State key laboratory for turbulence and complex systems, Peking University, Beijing, 100871, People's Republic of China and Joint Laboratory of Marine Hydrodynamics and Ocean Engineering, Laoshan Laboratory, Shandong 266237, People's Republic of China



(Received 6 December 2022; accepted 5 April 2023; published 21 April 2023)

We explore the spatial-temporal structure functions of Burgers turbulence driven by a temporal Ornstein-Uhlenbeck (OU) process, where the characteristic time scale of the OU process is much larger than that of the energy flux across spatial scales. Based on the Kármán-Howarth-Monin equation and the temporal scale separation, we postulate an expression for the third-order spatial-temporal structure function away from the dissipation scale. This expression combines Kolmogorov's exact result of spatial structure function and the exponential temporal decay of the external force. We numerically justify this expression and find that the high-order structure functions also decay exponentially; however, the dependence of decay rates on order is different for the odd- and even-order structure functions. Comparing the OU-driven Burgers turbulence with that driven by temporal white noise, their spatial structure functions are identical when the energy injection rates are the same, which justifies Kolmogorov's theory, but these two systems' temporal structure functions differ. Also, the velocity probability density function in the OU-driven Burgers turbulence shows a bimodal distribution, contradicting the near-Gaussian distribution in white-noise-driven turbulence. Even though we lack a rigorous and general derivation of the dependence of the third-order structure function on the temporal statistics of the driving force, our results imply that one can obtain forcing temporal statistics using measured temporal data. However, inferring energy flux across spatial scales solely based on temporal information seems impossible.

DOI: [10.1103/PhysRevFluids.8.044602](https://doi.org/10.1103/PhysRevFluids.8.044602)

I. INTRODUCTION

Turbulence, which involves complicated spatial-temporal information, is ubiquitous in natural and artificial fluid systems. Structure functions are widely used to describe and study spatial-temporal statistical features of turbulent systems [1]. By bridging measurable velocity structure functions with the physically important energy transfer rate across spatial scales, Kolmogorov's structure-function theory establishes a foundation for modern statistical turbulence theory. In 1999, Lindborg [2], Bernard [3], and Yakhot [4] developed the exact structure-function theory for two-dimensional turbulence. It differs from the theory for 3D turbulence by the coexistence of inverse kinetic and forward enstrophy cascades. Exact third-order structure function expressions were also derived in other turbulent systems, including Burgers turbulence [5–8], turbulence with bidirectional energy transfer [9–11], and anisotropic sheared turbulence [12–14].

*jinhanxie@pku.edu.cn

Exact expressions of structure functions in compressible turbulence are more complicated [15–19] because not only are there velocity structure functions, but also density- and pressure-related terms; thus, there coexists multiple modes with distinctive features [20]. High-order structure functions are also important for understanding turbulence statistics, however, in their governing equations the number of unknown independent variables is larger than the number of equations [21], leaving the expressions for high-order structure functions not explicitly solvable.

Structure functions, which consist of velocity difference at different times, capture turbulence temporal statistics. They are also key quantities calculated from measured data at fixed locations in natural turbulence, e.g., turbulence in the atmosphere [22], ocean [23], and outer space [24], where spatial information is sparse due to the limited number of instruments. To understand the temporal structure functions, one can identify the characteristic cascade time scale with the characteristic correlation time scale to deduce the temporal correlation based on Kolmogorov’s self-similarity assumption [25–29]. Under the assumption that small-scale eddies are randomly swept by large-scale eddies with negligible distortion, from a Lagrangian viewpoint, Kraichnan [30] proposed that the velocity correlation decays as a Gaussian of the temporal difference and the decay rate is scaledependent. The random sweeping assumption has been later checked in three-dimensional homogeneous isotropic turbulence [31–36]. Tennekes [37] argued that Kolmogorov’s self-similarity assumption applies to Lagrangian velocity. When a mean flow is present, Taylor [38] hypothesized that the mean flow carries the spatial structures of turbulent flow without much change, therefore, the spatial and temporal structure functions are linearly related. Combing the random sweeping and Taylor’s frozen hypothesis, He and Zhang [39] proposed the elliptic model, which states that the iso-correlation contours in the spatial-temporal difference domain are ellipses. Detailed information on spatial-temporal correlations in turbulent flows can be found in the review article [1].

Most turbulent systems are driven by temporal white-noise external forcing in the studies of (spatial) temporal structure functions. Nevertheless, in realistic scenarios, external forcing has characteristic time scales, such as the periodic tidal forcing in the ocean. Periodic forcing introduces periodic energy injection rates, and this scenario, named modulated turbulence, has been widely studied [40–47].

However, the modulated turbulence is not statistically steady, which distinguishes it from statistically steady states in traditional turbulence and brings about extra difficulties in deriving structure-function theories. So, for simplicity, we consider statistically steady external forcing with prescribed temporal correlation, specifically a temporal Ornstein-Uhlenbeck (OU) process, whose correlation decays exponentially. This enables us to study the dependence of structure function in statistically steady states on the external forcing time scale. The OU forcing was used to drive isotropic turbulence [48,49]. Particularly, Yeung and Pope [49] found that the Lagrangian second-order structure function inherits an exponential dependence on the OU forcing. Different from their work, this paper focuses on the Eulerian third-order structure function whose spatial dependence is derived from the Kármán-Howarth-Monin (KHM) equation [27,50,51], but the potential of the KHM equation in understanding temporal structure functions is less explored (cf. [52]).

In this paper, we study Burgers turbulence forced by an OU process for numerical simplicity. In Sec. II, we obtain the expression for the third-order structure function based on the KHM equation. Then we perform numerical simulations to justify the third-order structure function expression and study the high-order structure functions in Sec. III. The comparison between the OU-driven Burgers turbulence and that driven by temporal white-noise forcing is also presented. We summarize and discuss our results in Sec. IV.

II. THE THIRD-ORDER STRUCTURE FUNCTION

We start from the forced-dissipative Burgers equation

$$u_t + \frac{1}{2}\partial_x u^2 = F + D, \quad (1)$$

where F and D represent external forcing and dissipation, respectively.

In a statistically steady turbulent state, we consider two-point measurements at locations x and $x' = x + r$ with the displacement r , and two instances at t and $t' = t + \tau$ with temporal difference τ . By assuming homogeneity, we obtain

$$\partial_x = -\partial_{x'} = -\partial_r. \quad (2)$$

Steadiness implies

$$\partial_t = -\partial_{t'} = -\partial_\tau. \quad (3)$$

Multiplying $u' = u(x', t')$ with (1), adding the conjugate equation, and taking an average we obtain

$$-\frac{1}{6}\partial_r\overline{\delta u^3} = \overline{u'F} + \overline{uF'} + \overline{u'D} + \overline{uD'}, \quad (4)$$

where $\delta u = u' - u$ and the overbar $\bar{\cdot}$ denotes the average. Note that the time-derivative term is identically zero in a statistically steady state, and we arrive at a KHM equation that is identical to the one where the two measured points have no temporal difference.

When the external forcing is whitenoise in time, considering spatial displacement with $\tau = 0$, we have [cf. 53]

$$\overline{uF'} + \overline{u'F} = 2\overline{F'F}, \quad (5)$$

and therefore, the spatial third-order structure function becomes

$$\overline{\delta u^3}(r, 0) = -12 \int_0^r C(s)ds + \int_0^r (\overline{u'D} + \overline{uD'})dr, \quad (6)$$

where $\overline{F'F} = C(r)$ and $C(0) = \epsilon$ is the energy injection rate. Considering that energy transfers downscale, ignoring the effect of dissipation away from the dissipation scale, we obtain (cf. [54,55])

$$\overline{\delta u^3} = -12 \int_0^r C(s)ds, \quad (7)$$

which, in the limit of $r \rightarrow 0$, recovers the inertial-range result

$$\overline{\delta u^3} = -12\epsilon r. \quad (8)$$

When the external forcing F is not a white noise in time, the relation between energy injection and the correlation of the external forcing (5) does not hold, and we may not be able to obtain an explicit expression for the effect of external forcing in the KHM equation. This is because the temporal integration of the nonlinear term is not guaranteed to be small compared with the effect of forcing. However, when a temporal scale separation exists between the turbulent nonlinear effect and the forcing's correlation time, the relation (5) may still hold.

To study the turbulence response to a temporally correlated forcing, we consider a simple case where the external forcing F follows an OU process with temporal correlation

$$\overline{F'F} = C(r)e^{-\sigma|\tau|}, \quad (9)$$

where $C(r)$ is the externally prescribed forcing correlation and σ is the decay rate of the OU process.

But with a temporally correlated forcing, we do not have an exact relation such as (6). So we consider a scenario with temporal scale separation, where the characteristic time scale given by energy flux across spatial scales, $(k_f^2\epsilon)^{-1/3}$, is much smaller than the correlation time scale of the OU process, $1/\sigma$. Then we conjecture that at a time scale comparable with $1/\sigma$, the third-order structure function inherits the temporal dependence of the OU process. Thus, based on the knowledge of spatial structure function (7), we postulate

$$\overline{\delta u^3} = -12\epsilon e^{-\sigma|\tau|} \int_0^r \frac{C(s)}{C(0)} ds. \quad (10)$$

Note that when calculating the spatial structure function, based on the downscale energy flux, we can argue that the contribution of small-scale dissipation tends to zero as the viscosity tends to zero [51,56,57]. However, for the spatial-temporal structure function, we do not have a similar estimation for the dissipation effect, so we simply assume that with a fixed time scale the dissipation effect also tends to zero as the viscosity tends to zero.

Particularly, if the OU forcing only acts at one scale ($1/k_f$), i.e.,

$$F = F_0(A \cos(k_f x) + B \sin(k_f x)), \quad (11)$$

where F_0 is a constant. A and B are independent OU processes generated by

$$dA = -\sigma A dt + \sqrt{2\sigma} dW, \quad (12a)$$

$$dB = -\sigma B dt + \sqrt{2\sigma} dW, \quad (12b)$$

where dW is a white noise with variance one. Then the correlation of F becomes

$$\overline{FF'} = 2F_0^2 \sigma \cos(k_f r) e^{-\sigma|\tau|}. \quad (13)$$

Thus, (10) becomes

$$\overline{\delta u^3} = -12 \frac{\epsilon}{k_f} \sin(k_f r) e^{-\sigma|\tau|}, \quad (14)$$

which we justify in numerical results below. When $\tau = 0$, (14) recovers the forcing-scale resolving third-order structure function expression [11,56]; taking a further limit of $kr \ll 1$, the inertial-range result $\overline{\delta u^3} = -12\epsilon r$ is obtained [5,58–60].

III. NUMERICAL RESULTS

In this section, we run second-order finite-volume numerical simulations with a van Leer limiter in space and a fourth-order explicit Runge-Kutta scheme in time for the Burgers turbulence forced by the OU process and white noise. The resolution is 4096 in a periodic domain of size 2π . We add no explicit dissipation, and the injected energy is absorbed by the numerical dissipation by the finite-volume scheme to reach statistically steady states. A simulation for Burgers turbulence driven by temporal white-noise forcing is also performed as a comparison. The white-noise simulation is checked against theoretical results of forcing-scale-resolving spatial structure functions in [55]. In the OU-driven turbulence, we take $k_f = 3$ and $\sigma = 0.05$ [cf. (11) and (13)], and $\epsilon \approx 420$ is obtained from the statistically steady state by directly calculating the energy injection by external forcing. So the time scale separation between the OU process and energy flux across spatial scale is well satisfied with $(k_f^2 \epsilon)^{1/3} / \sigma \approx 300 \gg 1$.

In these simulations, the Burgers turbulences reach statistically steady states where statistical quantities are calculated. To obtain convergent spatial-temporal statistics, we consider a statistically steady state of a time interval of $400/\sigma$ with equipartitioned 80 000 snapshots. Thus, for each spatial and temporal displacement, the statistics are calculated over $4096 \times 79\,600$ data value. Here, $79\,600 = 80\,000 \times 398/400$ considering the maximum temporal difference considered is $2/\sigma$.

A. Structure functions in OU-driven Burgers turbulence

Figure 1 shows the spatial-temporal second- and third-order structure functions. The third-order structure function matches well with the expression (14), which we check in the following figures with more details. In this figure, we observe a slight odd signal in τ , i.e., $\tau \rightarrow -\tau$ asymmetry, but this asymmetry decreases as the interval used to perform statistics increases, so in Figs. 2 and 3 we only show the even parts of the structure functions.

In Fig. 2, we show the temporal dependence of second- and third-order correlations with fixed spatial displacements. In the left panel, the τ dependence of $2\overline{u'u} = 2\overline{u^2} - \overline{\delta u^2}$, normalized by its peak value, at $x = 0, \pi/12, 2\pi/12, 3\pi/12, 4\pi/12$, and $5\pi/12$ are presented. When $r = \pi/3$, the

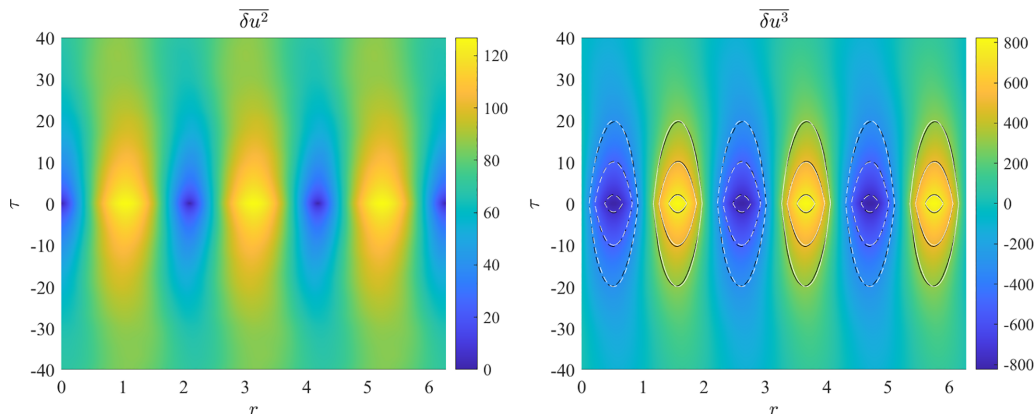


FIG. 1. Second- and third-order spatial-temporal structure functions in OU-driven Burgers turbulence. The black and white curves in the right panel are the contours of the numerical data and theoretical expression (14) at levels $\pm 12\epsilon e^{-0.1}/k_f$, $\pm 12\epsilon e^{-0.5}/k_f$ and $\pm 12\epsilon e^{-1}/k_f$. The solid and dashed curves mark the positive and negative values, respectively.

second-order correlation function reaches its peak value $\overline{u'u}(\pi/3, 0)$, and as the time difference increases, the second-order correlation function decorrelates following an exponential function, $e^{-\sigma|\tau|}$, which is inherited from the temporal decorrelation of the external forcing [cf. (13)]. When $r = \pi/6$, due to its near-zero value (cf. left panel of Fig. 1), the normalized correlation function differs from structure functions evaluated at other spatial displacements.

We present the temporal dependence of third-order structure functions with fixed spatial displacements in the right panel of Fig. 2. The fixed spatial displacements are taken as $x = \pi/12, 2\pi/12, 3\pi/12, 5\pi/12, 6\pi/12$, and $7\pi/12$, and they cover two peak values, at $x = \pi/6$ and $\pi/2$, for the absolute value of the third-order structure function. We find that these curves match the decorrelation $e^{-\sigma|\tau|}$ very well, which justifies our theoretical prediction (14).

We show the structure functions of different orders with fixed spatial displacements to quantitatively study the temporal correlations. In Fig. 2 we show that the second- and third-order structure functions with different displacements have the same temporal decay rate. However, high-order structure functions with different displacements have different temporal decay rates,

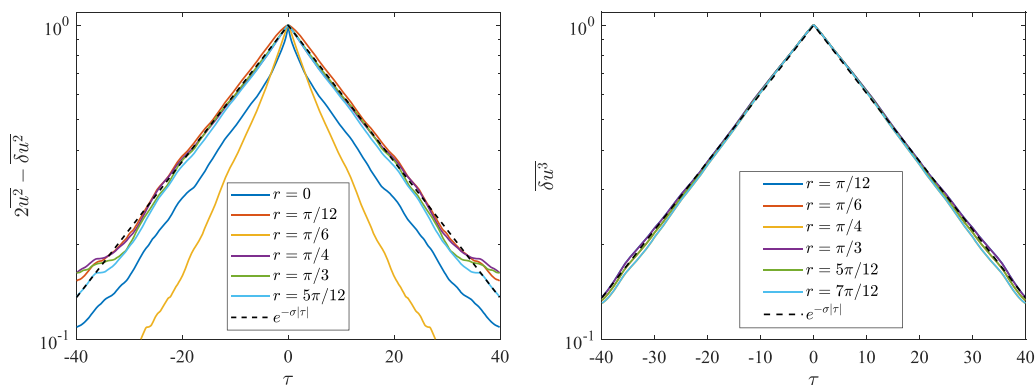


FIG. 2. Temporal dependence of the second- and third-order structure functions with different spatial displacements. The structure functions are normalized by their corresponding peak values at $\tau = 0$. The forcing correlation $e^{-\sigma|\tau|}$ is plotted as dashed curves for reference.

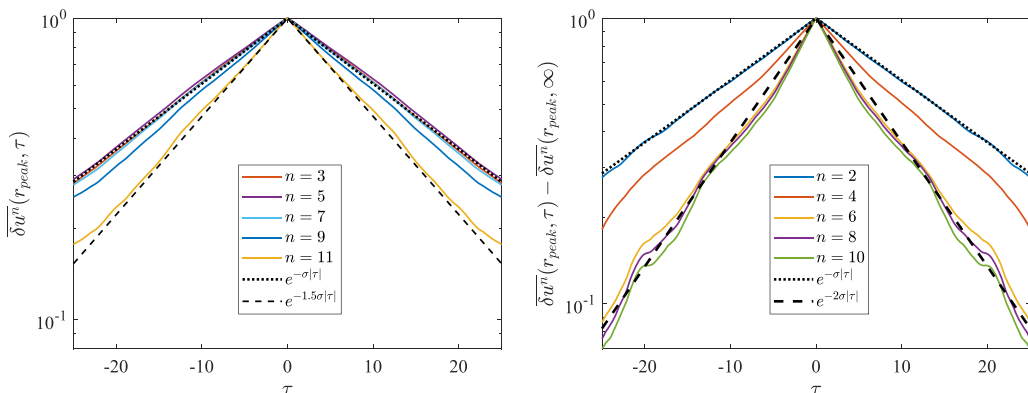


FIG. 3. Temporal dependence of odd- and even-order structure functions with fixed spatial displacements chosen at each peak along $\tau = 0$. Curves with decay rates σ , 1.5σ , and 2σ are plotted as references.

which we illustrate using the seventh-order structure function in Sec. III A. Thus, to capture the temporal dependence brought about by the external forcing, we consider the temporal decay of the structure function with displacement corresponding to the peak of structure functions along $\tau = 0$. Here, we fix the spatial displacements as the ones that take the peak value of the corresponding structure functions along $\tau = 0$, e.g., for the second- and third-order structure functions, the spatial displacements are taken as $r = \pi/3$ and $\pi/4$, respectively.

The left panel of Fig. 3 shows that the odd-order structure functions decay exponentially, which resembles the external forcing temporal correlation. For the low orders, $n = 3, 5, 7$, the decay rate is identical to the decay rate of the external forcing, σ . However, as the order increases, the decay rates increase. For the even orders, because the structure functions do not decay to zero as τ tends to ∞ , we plot $\overline{\delta u^n}(r_{\text{peak}}, \tau) - \overline{\delta u^n}(r_{\text{peak}}, \infty)$ in the right panel of Fig. 3 and find that they also decay exponentially. As the order increases, the decay rates increase and saturate to a decay rate of 2σ . We can obtain the value of $\overline{\delta u^n}(r_{\text{peak}}, \infty)$ because the nonzero structure functions at $\tau \rightarrow \infty$ are brought about by correlations in the form $u^\alpha(x+r, t+\tau)u^\beta(x, t)$ with α and β even integers. Considering that $u(x+r, t+\tau)$ and $u(x, t)$ are independent when $\tau \rightarrow \infty$, $\lim_{\tau \rightarrow \infty} \overline{u^\alpha(x+r, t+\tau)u^\beta(x, t)} = \overline{u^\alpha} \overline{u^\beta}$, e.g., $\overline{\delta u^4}(r_{\text{peak}}, \infty) = 2\overline{u^4} + 6(\overline{u^2})^2$.

We express the temporal decay of structure function with order n as $\overline{\delta u^n}(r_{\text{peak}}, \tau) - \overline{\delta u^n}(r_{\text{peak}}, \infty) \sim e^{-p_n \sigma |\tau|}$, where p_n measures the decay rate. The values of p_n are collected in Fig. 4. The convergence check of tenth- and eleventh-order statistics is shown in Sec. III B.

B. Comparing white-noise and OU-driven turbulence

As a comparison, we run a numerical simulation of Burgers turbulence driven by temporal white-noise external forcing, which has the same energy injection rate as that of the OU forcing.

First, we show the Hovmöller diagram for field u in two numerical simulations at statistically steady states in Fig. 5. Both panels show large-scale structures corresponding to forcing scale $k_f = 3$, while the field driven by OU forcing has a longer time correlation than that forced by temporal white noise.

In Fig. 6, we check the second- and third-order spatial structure functions. The coincidence of curves reveals the validity of Kolmogorov's scenario in spatial space due to the equal energy injection rate, and we cannot distinguish the two types of turbulence using spatial structure function. Also, the r scaling is consistent with the result driven by [5].

The spatial-temporal dependence of the second- and third-order structure functions is shown in Fig. 7. As expected, we observe that structure functions in Burgers turbulence driven by temporal

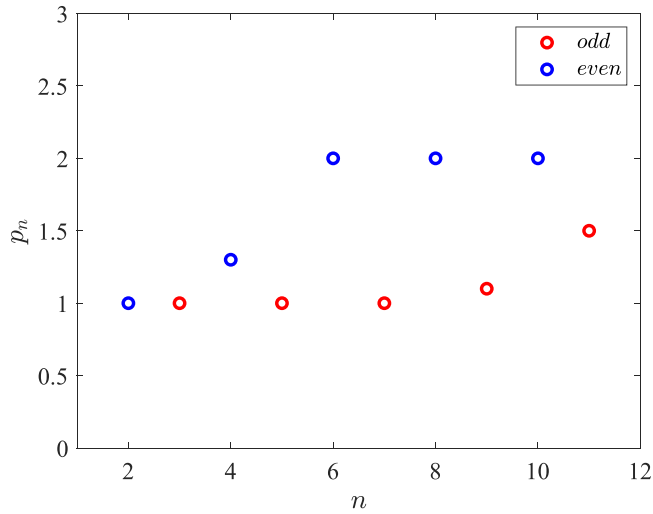


FIG. 4. The dependence of the decorrelation rate normalized by σ on the order of structure function.

white-noise forcing have much shorter time correlations than those forced by the OU process, which indicates that the long-time correlation in the latter scenario is a result of prescribed forcing. This short time correlation is shown in Fig. 8 by structure functions with fixed spatial displacement.

Finally, in Fig. 9, we compare the pdf of field u in statistically steady states with two types of forcing. When driven by temporal white noise, the pdf of u follows a normal distribution, but

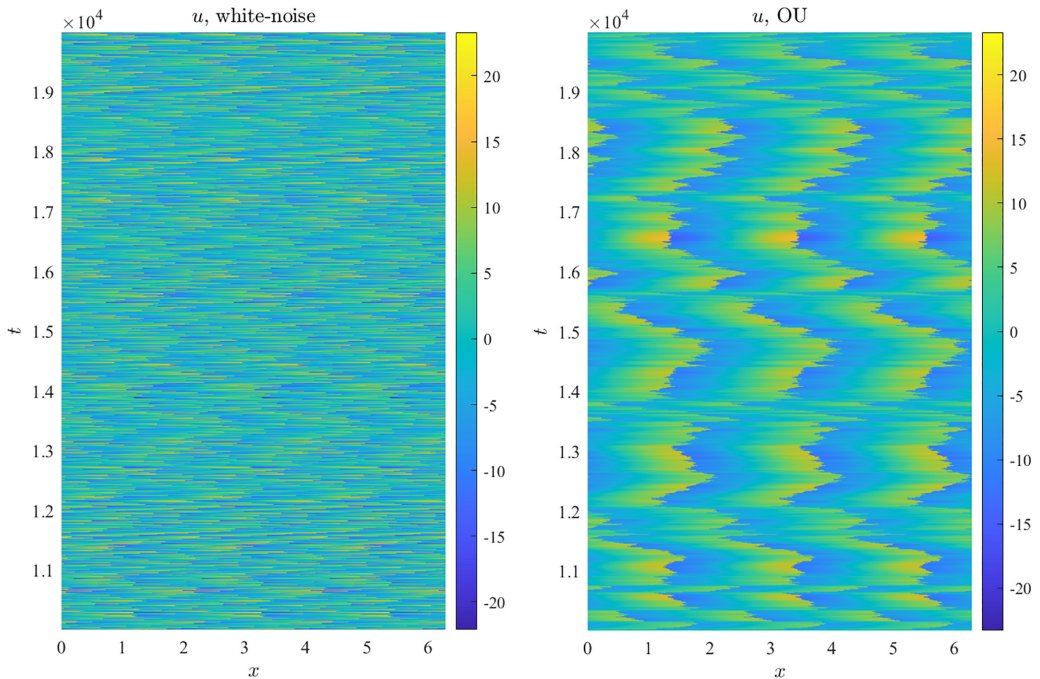


FIG. 5. Hovmöller diagram for u in Burgers turbulence driven by temporal white-noise and OU forcing, respectively.

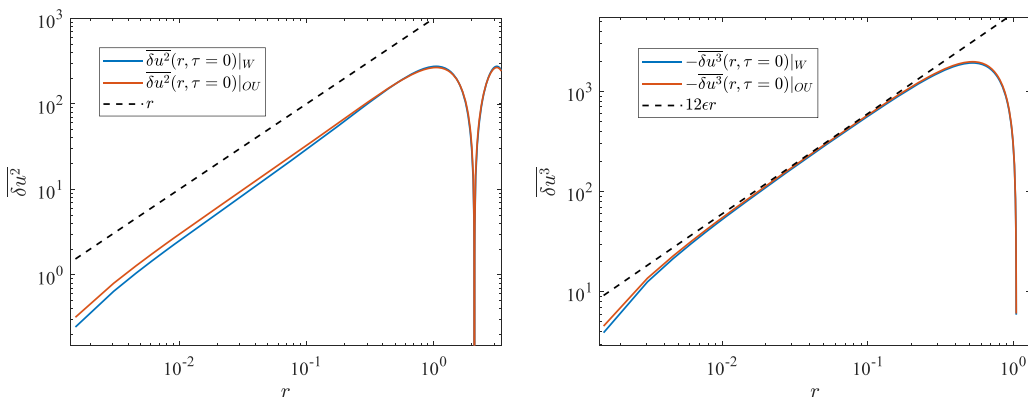


FIG. 6. Second- and third-order structure functions with $\tau = 0$ in Burgers turbulence driven by temporal white-noise and OU forcing.

a bimodal distribution is observed when forced by the OU process. This bimodal distribution resembles that in the truncated Burgers turbulence [61], where the “tygers” exist (cf. [62], for the flow structure “tyger”). However, different from the observation by [61] where the bimodal distribution is in transit, and the final distribution is close to Gaussian, our bimodal distribution is observed in a statistically steady state, which is a result of the OU forcing. We also need to note that the truncated Burgers system distinguishes from our system, and it remains to study whether there is a link between these two bimodal distributions.

IV. SUMMARY AND DISCUSSION

We explore the response of structure functions of Burgers turbulence driven by an OU process whose time scale is much larger than that of the energy flux across spatial scales, estimated by $k_f^{-2/3}\epsilon^{-1/3}$. Based on the KHM equation, we obtain an expression for the spatial-temporal third-order structure function, which combines the spatial dependence of the classic expression with the exponential temporal decay inherited from the external forcing. For the structure functions of other orders, we focus on the temporal dependence of structure functions evaluated at the peak for spatial displacement to capture the forcing impact. For the odd order, the external forcing’s exponential

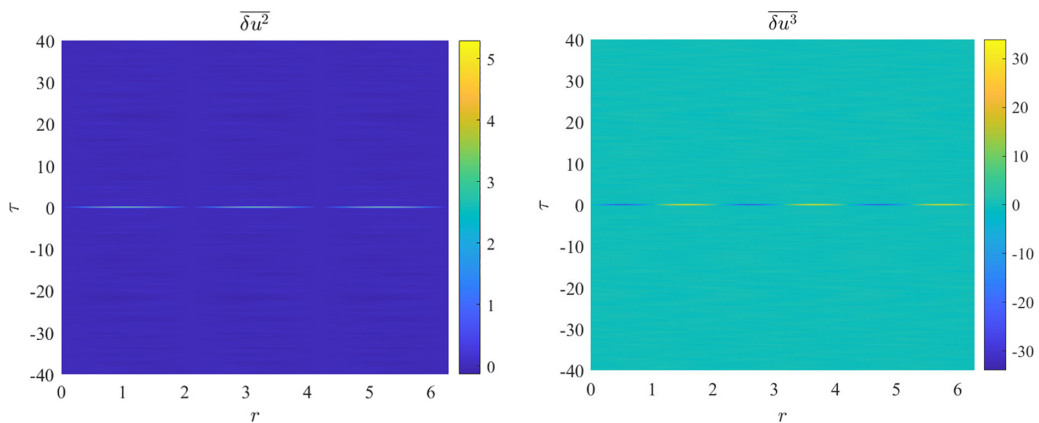


FIG. 7. Second- and third-order spatial-temporal structure functions in Burgers turbulence driven by temporal white-noise forcing.

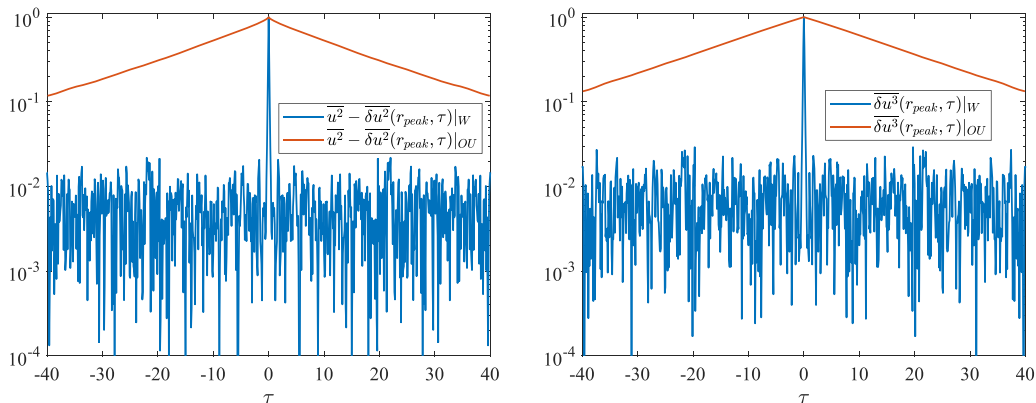


FIG. 8. Second- and third-order spatial-temporal structure functions with fixed spatial displacement in Burgers turbulence driven by temporal white-noise forcing. The spatial displacement for each structure function is picked so that when $\tau = 0$ the structure functions are at the peaks. All the structure functions are normalized by their own maximum values taken at $\tau = 0$.

decay rate is inherited by low-order structure function up to order seven, while for larger orders, the decay rate increases as the order increases. As to the even order, the second-order structure function decays at the decay rate of the external forcing, and then the decay rate increases and finally saturates at twice the external forcing's decay rate after order six. Here, since the even order structure function does not decay to zero, the decay rate is extracted from $\overline{\delta u^n}(r_{\text{peak}}, \tau) - \overline{\delta u^n}(r_{\text{peak}}, \infty)$.

In our OU-driven Burgers turbulence, the second-order structure function's exponential decay rate is the same for all spatial scales, making it different from the prediction by random sweeping [30], where the decorrelation is Gaussian and scale-dependent. This exponential decay agrees with the results calculated from the functional renormalization-group method [63], but we should distinguish these two results due to different external forcing. Also, the exponential decay agrees with the numerical discovery by Gorbunova *et al.* [36] at a large time difference, but we do not know if there is a link between these two results.

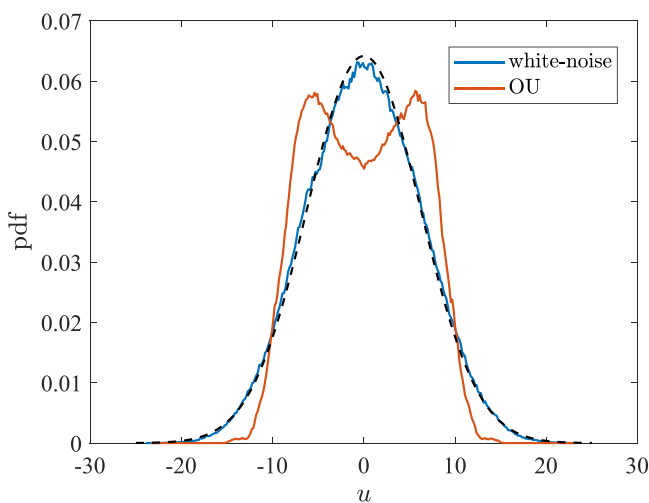


FIG. 9. Pdf of u in statistically steady Burgers turbulence driven by temporal white-noise and OU forcing. The black dashed line is a normal distribution for reference.

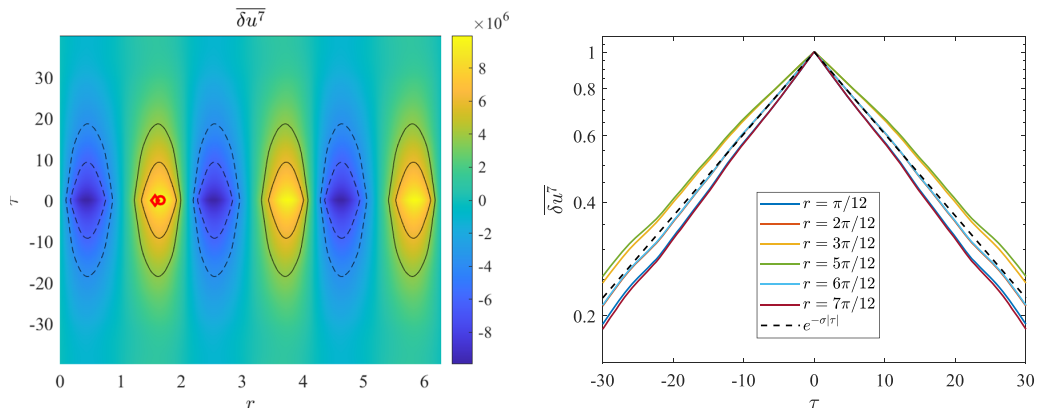


FIG. 10. Left: The spatial temporal seventh-order structure function. The black curves are the contours at levels $\pm \max\{\overline{\delta u^7}\}e^{-0.5}$ and $\pm \max\{\overline{\delta u^7}\}e^{-1}$ with the solid and dashed curves marking the positive and negative values, respectively. The red diamond and circles mark $(r, \tau) = (\pi/2, 0)$ and the point corresponding to the maximum value of $\overline{\delta u^7}$, respectively. Right: Temporal dependence of the seventh-order structure functions with different spatial displacements. The structure functions are normalized by their corresponding peak values at $\tau = 0$. The forcing correlation $e^{-\sigma|\tau|}$ is plotted as dashed curves for reference.

When comparing the Burgers turbulence driven by the OU process with that driven by temporal white-noise forcing with the same energy injection rate, we find that the spatial third-order structure functions are identical for the two systems, justifying Kolmogorov's theory. As to the pdf of u field, we find that the pdf in the OU-driven system has a symmetric bimodal distribution, contradicting the near-Gaussian distribution for the pdf in the temporal white-noise-driven turbulence. However, the reason behind this bimodal distribution has yet to be understood.

It needs to be noted that we do not derive the third-order structure-function expression but propose its form and justify it using numerical simulation. A rigorous derivation starting from stochastic differential equations is still required.

In addition, the exponential decay of the third-order structure function may be linked to the Lagrangian second-order structure function [64], considering that these two statistical quantities may amount to a time derivative. This link may be obtained from the velocity-acceleration correlation proposed by [65,66]. However, the nonlinear mapping between Lagrangian and Eulerian descriptions must be considered to express the above connection clearly.

Using the KHM equation to obtain or conjecture a third-order structure-function response to external temporal correlated forcing can be potentially generalized to other types of forcing. This paper only uses the OU process as a heuristic example. In our future work, we would follow a similar procedure to study the spatial-temporal structure functions in temporal correlated driven two- and three-dimensional turbulence.

Since for measurements in the atmosphere [22], ocean [23], and outer space [24] the temporal information is more resolved than spatial, it would be good that analytical expressions linking the spatial and temporal statistics exist. For the second-order statistics, e.g., the velocity correlation, the elliptic model is proposed based on the local maximum of the point at zero spatial and temporal displacement [1]; however, a similar idea does not apply to the third-order structure function, which links to the important energy flux across spatial scales. Our proposed third-order structure-function expression provides such a possibility. Even though not rigorously derived, it shows that forcing temporal statistics is important for the third-order structure function, and it seems impossible to infer spatial third-order structure function from temporal information alone.

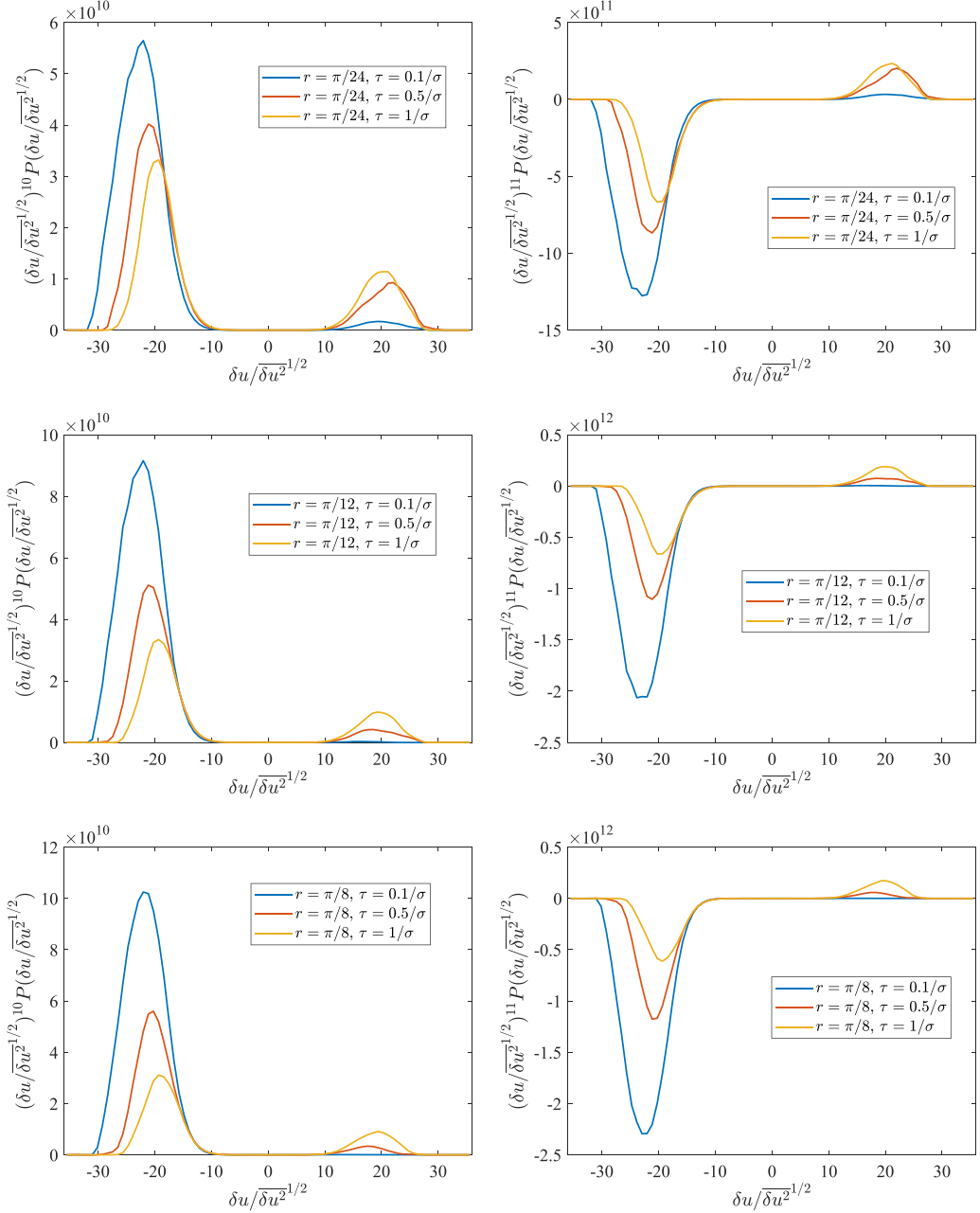


FIG. 11. $(\delta u / \delta u^2)^n P(\delta u / \delta u^2)^{1/2}$ with spatial displacement $r = \pi/24, \pi/12,$ and $\pi/8$; and temporal displacement $\tau = 0.1/\sigma, 0.5/\sigma,$ and $1/\sigma$. The left and right panels show the results of $n = 10$ and 11 , respectively.

ACKNOWLEDGMENTS

J.-H.X. thanks Prof. Qingdong Cai for helpful discussion on numerical schemes and acknowledges the financial support from the Natural Science Foundation of China (NSFC) under Grants No. 92052102 and No. 12272006, and Laoshan Laboratory under Grant No. LSKJ202202000.

APPENDIX A: THE SEVENTH-ORDER SPATIAL TEMPORAL STRUCTURE FUNCTION

When the orders are higher than three, the temporal dependence of structure functions differ for different displacements; therefore, when we compare the temporal dependence of structure functions of different orders in the main text, we choose the temporal structure functions with displacement corresponding to the peak of them along $\tau = 0$. In Fig. 10, we illustrate this phenomenon using the seventh-order structure function. In the left panel, we show that the spatial seventh-order structure function with $\tau = 0$ is not captured by the $\sin k_f r$, which is a theoretical result for the third-order structure function, and the right panel shows that with different spatial displacement the temporal decay rates differ.

APPENDIX B: CONVERGENCE OF HIGH-ORDER STRUCTURE FUNCTIONS

To check the convergence of high-order statistics of the OU-driven Burgers turbulence, Fig. 11 plots $(\delta u / \overline{\delta u^2})^n P(\delta u / \overline{\delta u^2})$ with $n = 10$ and 11. Here, P is the pdf function.

-
- [1] G. He, G. Jin, and Y. Yang, Space-time correlations and dynamic coupling in turbulent flows, *Annu. Rev. Fluid Mech.* **49**, 51 (2017).
 - [2] E. Lindborg, Can the atmospheric kinetic energy spectrum be explained by two-dimensional turbulence? *J. Fluid Mech.* **388**, 259 (1999).
 - [3] D. Bernard, Three-point velocity correlation functions in two-dimensional forced turbulence, *Phys. Rev. E* **60**, 6184 (1999).
 - [4] V. Yakhot, Two-dimensional turbulence in the inverse cascade range, *Phys. Rev. E* **60**, 5544 (1999).
 - [5] W. E and E. Vanden Eijnden, Asymptotic Theory for the Probability Density Functions in Burgers Turbulence, *Phys. Rev. Lett.* **83**, 2572 (1999).
 - [6] G. Falkovich and K. R. Sreenivasan, Lessons from hydrodynamic turbulence, *Phys. Today* **59**(4), 43 (2006).
 - [7] J. Cardy, G. Falkovich, and K. Gawedzki, *Non-Equilibrium Statistical Mechanics and Turbulence* edited by S. Nazarenko and O. V. Zaboronski (Cambridge University Press, 2008).
 - [8] G. Falkovich, *Fluid Mechanics: A Short Course for Physicists* (Cambridge University Press, 2011).
 - [9] A. Alexakis and L. Biferale, Cascades and transitions in turbulent flows, *Phys. Rep.* **767-769**, 1 (2018).
 - [10] J.-H. Xie and O. Bühler, Two-dimensional isotropic inertia-gravity wave turbulence, *J. Fluid Mech.* **872**, 752 (2019).
 - [11] J.-H. Xie and O. Bühler, Third-order structure functions for isotropic turbulence with bidirectional energy transfer, *J. Fluid Mech.* **877**, R3 (2019).
 - [12] C. M. Casciola, P. Gualtieri, R. Benzi, and R. Piva, Scale-by-scale budget and similarity laws for shear turbulence, *J. Fluid Mech.* **476**, 105 (2003).
 - [13] M. Wan, S. Servidio, S. Oughton, and W. H. Matthaeus, The third-order law for increments in magnetohydrodynamic turbulence with constant shear, *Phys. Plasmas* **16**, 090703 (2009).
 - [14] M. Wan, S. Servidio, S. Oughton, and W. H. Matthaeus, The third-order law for magnetohydrodynamic turbulence with shear: Numerical investigation, *Phys. Plasmas* **17**, 052307 (2010).
 - [15] S. Galtier and S. Banerjee, Exact Relation for Correlation Functions in Compressible Isothermal Turbulence, *Phys. Rev. Lett.* **107**, 134501 (2011).
 - [16] J. Wang, Y. Yang, Y. Shi, Z. Xiao, X. T. He, and S. Chen, Cascade of Kinetic Energy in Three-Dimensional Compressible Turbulence, *Phys. Rev. Lett.* **110**, 214505 (2013).
 - [17] S. Banerjee and S. Galtier, A kolmogorov-like exact relation for compressible polytropic turbulence, *J. Fluid Mech.* **742**, 230 (2014).
 - [18] S. Chen, Z. Xia, J. Wang, and Y. Yang, Recent progress in compressible turbulence, *Acta Mech Sin* **31**, 275 (2015).
 - [19] B. Sun, Scaling laws of compressible turbulence, *Appl. Math. Mech. -Engl. Ed.* **38**, 765 (2017).

- [20] S. Chen, J. Wang, Q. Zheng, X. Wang, J. Teng, and M. Wan, Multi-scale analyses of compressible turbulence, *Acta Aerodynamica Sinica* **39**, 1 (2021).
- [21] R. J. Hill, Equations relating structure functions of all orders, *J. Fluid Mech.* **434**, 379 (2001).
- [22] G. Wang and X. Zheng, Very large scale motions in the atmospheric surface layer: a field investigation, *J. Fluid Mech.* **802**, 464 (2016).
- [23] A. C. Naveira Garabato, X. Yu, J. Callies, R. Barkan, K. L. Polzin, E. E. Frajka-Williams, C. E. Buckingham, and S. M. Griffies, Kinetic energy transfers between mesoscale and submesoscale motions in the open ocean's upper layers, *J. Phys. Oceanogr.* **52**, 75 (2022).
- [24] R. Marino and L. Sorriso-Valvo, Scaling laws for the energy transfer in space plasma turbulence, *Phys. Rep.* **1006**, 1 (2023).
- [25] S. Corrsin, Estimates of the relations between eulerian and lagrangian scales in large Reynolds number turbulence, *J. Atmos. Sci.* **20**, 115 (1963).
- [26] H. Tennekes and J. L. Lumley, *A First Course in Turbulence* (The MIT Press Cambridge, Massachusetts, and London, England, 1972).
- [27] A. S. Monin and A. M. Yaglom, *Statistical Fluid Mechanics, Volume II: Mechanics of Turbulence* (reprinted 2007) (Dover, Mineola, New York, 1975).
- [28] L. D. Landau and E. M. Lifshitz, *Fluid Mechanics*, 2nd ed. (Elsevier, Butterworth Heinemann, Amsterdam, Boston, 2010).
- [29] J. J. Podesta, Spatial scales and temporal scales in the theory of magnetohydrodynamic turbulence, *Phys. Plasmas* **18**, 012906 (2011).
- [30] R. H. Kraichnan, Kolmogorov hypotheses and eulerian turbulence theory, *Phys. Fluids* **7**, 1723 (1964).
- [31] S. A. Orszag and G. S. Patterson, Numerical Simulation of Three-Dimensional Homogeneous Isotropic Turbulence, *Phys. Rev. Lett.* **28**, 76 (1972).
- [32] S. Chen and R. H. Kraichnan, Sweeping decorrelation in isotropic turbulence, *Phys. Fluids A* **1**, 2019 (1989).
- [33] T. Sanada and V. Shanmugasundaram, Random sweeping effect in isotropic numerical turbulence, *Phys. Fluids* **4**, 1245 (1992).
- [34] Y. Kaneda, T. Ishihara, and K. Gotoh, Taylor expansions in powers of time of Lagrangian and Eulerian two-point two-time velocity correlations in turbulence, *Phys. Fluids* **11**, 2154 (1999).
- [35] L. Chevillard, S. G. Roux, E. Lévêque, N. Mordant, J.-F. Pinton, and A. Arnéodo, Intermittency of Velocity Time Increments in Turbulence, *Phys. Rev. Lett.* **95**, 064501 (2005).
- [36] A. Gorbunova, G. Balarac, L. Canet, G. Eyink, and V. Rossetto, Spatio-temporal correlations in three-dimensional homogeneous and isotropic turbulence, *Phys. Fluids* **33**, 045114 (2021).
- [37] H. Tennekes, Eulerian and Lagrangian time microscales in isotropic turbulence, *J. Fluid Mech.* **67**, 561 (1967).
- [38] G. I. Taylor, The spectrum of turbulence, *Proc. R. Soc. London A* **164**, 476 (1938).
- [39] G.-W. He and J.-B. Zhang, Elliptic model for space-time correlations in turbulent shear flows, *Phys. Rev. E* **73**, 055303(R) (2006).
- [40] D. Lohse, Periodically kicked turbulence, *Phys. Rev. E* **62**, 4946 (2000).
- [41] A. von der Heydt, S. Grossmann, and D. Lohse, Response maxima in modulated turbulence, *Phys. Rev. E* **67**, 046308 (2003).
- [42] A. von der Heydt, S. Grossmann, and D. Lohse, Response maxima in modulated turbulence. II. Numerical simulations, *Phys. Rev. E* **68**, 066302 (2003).
- [43] O. Cadot, J. H. Titon, and D. Bonn, Experimental observation of resonances in modulated turbulence, *J. Fluid Mech.* **485**, 161 (2003).
- [44] A. K. Kuczaj, B. J. Geurts, and D. Lohse, Response maxima in time-modulated turbulence: Direct numerical simulations, *Europhys. Lett.* **73**, 851 (2006).
- [45] W. J. T. Bos, T. T. Clark, and R. Rubinstein, Small scale response and modeling of periodically forced turbulence, *Phys. Fluids* **19**, 055107 (2007).
- [46] A. K. Kuczaj, B. J. Geurts, D. Lohse, and W. van de Water, Turbulence modification by periodically modulated scale-dependent forcing, *Computers & Fluids* **37**, 816 (2008).

- [47] H. E. Cekli, C. Tipton, and W. van de Water, Resonant Enhancement of Turbulent Energy Dissipation, [Phys. Rev. Lett. **105**, 044503 \(2010\)](#).
- [48] V. Eswaran and S. B. Pope, An examination of forcing in direct numerical simulations of turbulence, [Computers & Fluids **16**, 257 \(1988\)](#).
- [49] P. K. Yeung and S. B. Pope, Lagrangian statistics from direct numerical simulations of isotropic turbulence, [J. Fluid. Mech. **207**, 531 \(1989\)](#).
- [50] A. N. Kolmogorov, Dissipation of energy in locally isotropic turbulence, [Proc. R. Soc. Lond. A **434**, 15 \(1890\)](#).
- [51] U. Frisch, *Turbulence: the legacy of A. N. Kolmogorov* (Cambridge University Press, Cambridge, New York, 1995).
- [52] R. J. Hill, Opportunities for use of exact statistical equations, [J. Turbul. **7**, N43 \(2006\)](#).
- [53] K. Srinivasan and W. R. Young, Zonostrophic instability, [J. Atmos. Sci. **69**, 1633 \(2012\)](#).
- [54] J. Bec and K. Khanin, Burgers turbulence, [Phys. Rep. **447**, 1 \(2007\)](#).
- [55] J.-H. Xie, Sglobal expressions for high-order structure functions in burgers turbulence, [Acta Mech. Sin. **38**, 321132 \(2022\)](#).
- [56] J. Bec, U. Frish, and K. Khanin, Kicked burgers turbulence, [J. Fluid Mech. **416**, 239 \(2000\)](#).
- [57] J.-H. Xie and O. Bühler, Exact third-order structure functions for two-dimensional turbulence, [J. Fluid Mech. **851**, 672 \(2018\)](#).
- [58] W. E, K. Khanin, A. Mazel, and Y. Sinai, Probability Distribution Functions for the Random Forced Burgers Equation, [Phys. Rev. Lett. **78**, 1904 \(1997\)](#).
- [59] W. E, K. Khanin, A. Mazel, and Y. Sinai, Invariant measures for burgers equation with stochastic forcing, [Ann. Math. **151**, 877 \(2000\)](#).
- [60] E. Lindborg, A note on acoustic turbulence, [J. Fluid Mech. **874**, R2 \(2019\)](#).
- [61] P. Clark Di Leoni, P. D. Mininni, and M. E. Brachet, Dynamics of partially thermalized solutions of the burgers equation, [Phys. Rev. Fluids **3**, 014603 \(2018\)](#).
- [62] S. S. Ray, U. Frisch, S. Nazarenko, and T. Matsumoto, Resonance phenomenon for the galerkin-truncated burgers and euler equations, [Phys. Rev. E **84**, 016301 \(2011\)](#).
- [63] M. Tarpin, L. Canet, and N. Wschebor, Breaking of scale invariance in the time dependence of correlation functions in isotropic and homogeneous turbulence, [Phys. Fluids **30**, 055102 \(2018\)](#).
- [64] P. K. Yeung, Lagrangian investigations of turbulence, [Annu. Rev. Fluid Mech. **34**, 115 \(2002\)](#).
- [65] J. Mann, S. Ott, and J. S. Anderson, Experimental study of relative, turbulent diffusion, Denmark. Forskningscenter Risoe. Risoe-R No. 1036(EN), 1999.
- [66] S. Ott and J. Mann, An experimental investigation of the relative diffusion of particle pairs in three-dimensional turbulent flow, [J. Fluid Mech. **422**, 207 \(2000\)](#).